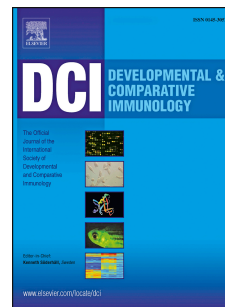


Accepted Manuscript

Fish-derived antimicrobial peptides: Activity of a chionodracine mutant against bacterial models and human bacterial pathogens

Francesco Buonocore, Simona Picchietti, Fernando Porcelli, Giulia Della Pelle, Cristina Olivieri, Elia Poerio, Francesca Bugli, Giulia Menchinelli, Maurizio Sanguinetti, Alberto Bresciani, Nadia Gennari, Anna Rita Taddei, Anna Maria Fausto, Giuseppe Scapigliati



PII: S0145-305X(18)30630-X

DOI: <https://doi.org/10.1016/j.dci.2019.02.012>

Reference: DCI 3348

To appear in: *Developmental and Comparative Immunology*

Received Date: 28 December 2018

Revised Date: 7 February 2019

Accepted Date: 15 February 2019

Please cite this article as: Buonocore, F., Picchietti, S., Porcelli, F., Della Pelle, G., Olivieri, C., Poerio, E., Bugli, F., Menchinelli, G., Sanguinetti, M., Bresciani, A., Gennari, N., Taddei, A.R., Fausto, A.M., Scapigliati, G., Fish-derived antimicrobial peptides: Activity of a chionodracine mutant against bacterial models and human bacterial pathogens, *Developmental and Comparative Immunology* (2019), doi: <https://doi.org/10.1016/j.dci.2019.02.012>.

This is a PDF file of an unedited manuscript that has been accepted for publication. As a service to our customers we are providing this early version of the manuscript. The manuscript will undergo copyediting, typesetting, and review of the resulting proof before it is published in its final form. Please note that during the production process errors may be discovered which could affect the content, and all legal disclaimers that apply to the journal pertain.

Fish-derived antimicrobial peptides: activity of a chionodracine mutant against bacterial models and human bacterial pathogens

Francesco Buonocore^{1*o}, Simona Picchietti^{1o}, Fernando Porcelli¹, Giulia Della Pelle¹, Cristina Olivieri^{1,2}, Elia Poerio¹, Francesca Bugli^{3,4}, Giulia Menchinelli^{3,4}, Maurizio Sanguinetti^{3,4}, Alberto Bresciani⁵, Nadia Gennari⁵, Anna Rita Taddei⁶, Anna Maria Fausto¹, Giuseppe Scapigliati¹

¹*Department for Innovation in Biological, Agrofood and Forest Systems, University of Tuscia, Viterbo (Italy)*

²*Department of Biochemistry, Molecular Biology and Biophysics, University of Minnesota, Minneapolis, 55455 USA*

³*Dipartimento di Scienze di Laboratorio e Infettivologiche, Fondazione Policlinico Universitario "A. Gemelli" IRCCS, Rome, Italy*

⁴*Istituto di Microbiologia, Università Cattolica del Sacro Cuore, Rome, Italy*

⁵*IRBM Science Park SpA, Biology Department, Rome (Italy)*

⁶*Center of Large Equipments, Section of Electron Microscopy, University of Tuscia, Viterbo (Italy)*

^oThese two Authors contributed equally to the paper

*Corresponding author at: Department for Innovation in Biological, Agro-food and Forest systems, University of Tuscia, Largo dell'Università snc, 05100 Viterbo (VT), Italy, E-mail address: fbuono@unitus.it

30
31
32
33
34
35
36
37
38
39
40
41
42
43
44
45
46
47
48
49
50
51
52
53
54
55

Francesco Buonocore: fbuono@unitus.it

Simona Picchietti: picchietti@unitus.it

Fernando Porcelli: porcelli@unitus.it

Giulia Della Pelle: giulia.dellapelle@studenti.unitus.it

Cristina Olivieri: colivier@umn.edu

Elia Poerio: poerio@unitus.it

Francesca Bugli: fra.bugli@gmail.com

Giulia Menchinelli: giulia.menchinelli@hotmail.it

Maurizio Sanguinetti: maurizio.sanguinetti@unicatt.it

Alberto Bresciani: A.Bresciani@irbm.it

Nadia Gennari: n.gennari@irbm.it

Anna Rita Taddei: artaddei@unitus.it

Anna Maria Fausto: fausto@unitus.it

Giuseppe Scapigliati: scapigg@unitus.it

56 **Abstract**

57 The increasing resistance to conventional antibiotics is an urgent problem that can be addressed by
58 the discovery of new antimicrobial drugs such as antimicrobial peptides (AMPs). AMPs are
59 components of innate immune system of eukaryotes and are not prone to the conventional
60 mechanisms that are responsible of drug resistance. Fish are an important source of AMPs and,
61 recently, we have isolated and characterized a new 22 amino acid residues peptide, the
62 chionodracine (Cnd), from the Antarctic icefish *Chionodraco hamatus*. In this paper we focused on
63 a new Cnd-derived mutant peptide, namely Cnd-m3a, designed to improve the selectivity against
64 prokaryotic cells and the antimicrobial activity against human pathogens of the initial Cnd template.
65 Cnd-m3a was used for immunization of rabbits, which gave rise to a polyclonal antibody able to
66 detect the peptide. The interaction kinetic of Cnd-m3a with the Antarctic bacterium *Psychrobacter*
67 sp. (TAD1) was imaged using a transmission electron microscopy (TEM) immunogold method.
68 Initially the peptide was associated with the plasma membrane, but after 180 min of incubation, it
69 was found in the cytoplasm interacting with a DNA target inside the bacterial cells. Using
70 fluorescent probes we showed that the newly designed mutant can create pores in the outer
71 membrane of the bacteria *E. coli* and *Psychrobacter* sp. (TAD1), confirming the results of TEM
72 analysis. Moreover, *in vitro* assays demonstrated that Cnd-m3a is able to bind lipid vesicles of
73 different compositions with a preference toward negatively charged ones, which mimics the
74 prokaryotic cell. The Cnd-m3a peptide showed quite low hemolytic activity and weak cytotoxic
75 effect against human primary and tumor cell lines, but high antimicrobial activity against selected
76 Gram – human pathogens. These results highlighted the high potential of the Cnd-m3a peptide as a
77 starting point for developing a new human therapeutic agent.

78

79

80

81 **Key words:** antimicrobial peptides; chionodracine mutant; antibody production; interaction with
82 bacterial membranes; antibacterial activity.

83

84

85

86

87

88

INTRODUCTION89
90
91
92
93
94
95
96
97
98
99
100
101
102
103
104
105
106
107
108
109
110
111
112
113
114
115
116
117
118
119
120

The antimicrobial peptides (AMPs), fundamental components of the innate immune system of prokaryotes and eukaryotes, have a broad specificity towards different pathogens, like bacteria, fungi, parasites and viruses (Zasloff M., 2002; Bulet et al., 2004). AMPs show different size, structure and physico-chemical characteristics and, therefore, can be classified based on their biosynthesis, their biological activities or their structural properties (α -helices, β -sheets, extended or loop structures) (Campagna et al., 2007). The AMPs usually, show amphipathic features with a positively charged, and a non-polar face, that are fundamental for their interaction with the anionic group present on the bacterial cell membrane (White and Wimley, 1998). They have been investigated from some time in clinical research as new antibiotics for infectious conditions caused by multidrug-resistant microbes (Hancock and Lehrer, 1998), but only few AMPs, until now, have been approved for clinical use, like polymyxins in the treatment of Gram – bacterial infections (Zavascki et al., 2007; Mahlapuu et al. 2016).

Fish live in an aquatic environment rich in microbial load and, therefore, their innate immune system rely highly on AMPs. Many different peptides have been isolated from fish in the last thirty years showing various biological activities (see the reviews of Ravichandran et al., 2010; Rajanbabu and Chen, 2011; Shabir et al., 2018). They comprise molecules belonging to the defensin, cathelicidin and hepcidin families, and also a specific family found only in fish and called piscidin (homologous to cecropin) (Noga and Silphaduang, 2003). Fish AMPs are active against both bacterial and virus fish specific pathogens (Pan et al., 2007; Chia et al., 2010) and some are also involved in iron regulation (Shi and Camus, 2006). Piscidins have been firstly isolated from mast cells of hybrid striped bass as different isoforms (piscidins 1, 2 and 3) (Noga and Silphaduang, 2003) and, successively, piscidin-like peptides have been found in sea bream stored in granules of professional phagocytic granulocytes (Mulero et al., 2008). Piscidin 2 is active against fish ectoparasites (Colorni et al., 2008) and, more recently, a new piscidin isoform (piscidin 4), involved in the killing of different fish bacterial pathogens, has been identified in the gills of hybrid striped bass (Corrales et al., 2009). Piscidins are produced as pre-pro-peptides and then activated, after cleavage, into a biologically active cationic molecule (about 22 amino acids in length); their pore-forming activity on bacterial cell wall is more likely achieved by a toroidal mechanism (Campagna et al., 2007), but recent results suggest that transient distortions of the membrane bilayer rather stable pores are responsible for membrane disruption (Perrin et al., 2016). Piscidin-like antimicrobial peptides have shown also interesting potential applications as chemotherapeutic drugs

121 due to their cytotoxic activity against breast cancer cells (Hilchie et al, 2011) and human
122 fibrosarcoma, histiocytic lymphoma and epithelial carcinoma (Hsu et al., 2011).

123 We have identified a piscidin-like AMP from the icefish (*Chionodraco hamatus*)
124 (Buonocore et al., 2012), an Antarctic teleost of the Channichthyidae family, and we have
125 determined its localization in gill mast cells and its antimicrobial activity against two
126 psychrotolerant and psychrophilic bacterial strains (*Psychrobacter* sp. TAD1 and TAD144). This 22
127 amino acid residues long peptide, named chionodracine (Cnd), did not show both significant lytic
128 activity on human erythrocytes and antimicrobial activity against human bacterial pathogens.
129 Successively, we have demonstrated that chionodracine is able to make discrete pores on the
130 membranes of both *Psychrobacter* sp. TAD1 and *Escherichia coli*, and that it folds into an
131 amphipathic α -helix in the presence of lipid vesicles (Olivieri et al., 2015). In this work, we
132 designed a new mutant starting from the sequence of the Cnd, namely Cnd-m3, with the aim to
133 improve its antimicrobial activity against human pathogens. We produced an antibody against this
134 new generated peptide that was used to investigate its internalization within bacterial membranes by
135 transmission electron microscopy (TEM). Moreover, we studied its ability to form pores on
136 *Psychrobacter* sp. TAD1 and *Escherichia coli* membranes and its binding capacity on lipid vesicles
137 mimicking bacterial membranes. Finally, we determined the Cnd-m3 hemolytic activity and
138 cytotoxic effect against human primary and cancer cell lines, and its antimicrobial activity against
139 both Gram – and Gram + human pathogens to assess its potential use as a new therapeutic drug.

140

141

142

143

144

145

146

147

148

149

150

MATERIALS AND METHODS151
152
153
154
155
156
157
158
159
160
161
162
163
164
165
166
167
168
169
170
171
172
173
174
175
176
177
178
179
180
181
182
183**2.1 Peptide and lipids**

The peptide (98% purity) was purchased from United Biosystem Inc. USA. Peptide concentration was determined for each sample preparation by UV light absorption at 280 nm. All lipids were purchased from Avanti Polar Lipids (Alabaster, AL, USA). The alignment between Cnd and Cnd-m3a was performed using Clustal Omega (<https://www.ebi.ac.uk/Tools/msa/clustalo/>). The net charge and the hydrophobic moment of the peptide have been calculated using the prediction tools of the APD3 Antimicrobial Peptide Database (<http://aps.unmc.edu>).

2.2 Antibody production and ELISA assay testing

The two synthetic mutant peptides (KS-Cnd NH₂-WFGHLYRGITKVVKHVHGLLLKG-COOH, see Olivieri et al., 2018, and Cnd-m3a NH₂-WFGKLYRGKTKVVKVKKVGLLLKG-COOH) were employed as antigens to immunize two New Zealand rabbits for obtaining anti-peptides antisera by a Company (Primm Srl, Milano, Italy). The immunization was performed subcutaneously with the two synthetic peptides conjugated to KLH, resuspended in 0.1M phosphate buffered saline (PBS) and with the use of complete Freund's adjuvant (Serva, Heidelberg, Germany) in the first two inoculi.

The obtained rabbit sera were tested in indirect ELISA against adsorbed immunization peptide Cnd-m3a. Briefly, lyophilized peptide was resuspended in distilled water at 30 µg/ml, and polystyrene wells were coated with 100 µl/well of peptide at a final concentration of 300 ng/well in 0.05 M carbonate-bicarbonate buffer pH 9.4. The wells were then washed three times with Tris-HCl 50 mM pH 7.4 containing 0.05% Tween-20 and 0.15 M NaCl (TTN). After blocking remaining sites with 3% BSA in TTN (TBT), 100 µl/well of the two antisera Peps1 and Peps2, separately diluted at 1:10, 1:100, 1:1000, 1:5000 in TBT, were added, incubating the plates for 3 hours at 4°C. Each experimental point was analysed in triplicate and control wells without adsorbed antigen were used as a control. The wells were carefully washed with TTN and then incubated for 2 hours with a HRP-conjugated anti-rabbit Ig secondary antibody solution (Cappel) in TBT. The wells were then washed with 50 mM phosphate-citrate buffer (pH 5.0) and the reaction was visualised using *o*-phenylenediamine (Sigma) as substrate. The absorbance values were read at 450 nm with an automatic plate reader (Labsystems). Optical density values (OD at 450 nm) of control wells were automatically subtracted from positive wells and the ELISA assays data have been calculated as the mean absorbance ± SD of the triplicate wells.

184 **2.3 Immunoelectron microscopy**

185 *Psychrobacter sp.* TAD1 bacteria cells were grown to the mid-log phase in Luria Bertani (LB broth
186 from Sigma) medium. Cnd-m3a peptide at a concentration of 15.0 μ M was added to the cultures
187 and they were incubated at different time points (0, 10 and 180 min at 15 °C) with shaking. At the
188 end of the incubation time, samples were centrifuged (5,000 rpm for 5 min) and the supernatant was
189 discarded. Samples at time 0, 10 and 180 minutes after incubation and untreated bacteria were
190 collected and fixed with 100 μ l of a mixture of 0.5% glutaraldehyde and 4% paraformaldehyde in
191 0.1 M phosphate buffer, pH 6.9, for 20 min at room temperature. After rinsing in the same buffer
192 for 10 min, samples were dehydrated in a graded ethanol series and embedded in medium grade LR
193 White resin. The resin was polymerised in tightly capped gelatine capsules for 24 h at 50°C.
194 Ultrathin sections were obtained using a Reichert Ultracut ultramicrotome with a diamond knife,
195 and collected on nickel grids.

196 For immunogold staining (IGS) non-specific antigens were blocked with 0.5% BSA in 0.05 M
197 TRIS-HCl buffer, pH 7.6 for 15 min. Sections were incubated overnight in a moist chamber with
198 the polyclonal antibody Peps2 diluted 1:100 in TRIS-HCl buffer, pH 7.6. The grids were washed in
199 0.05 M TRIS-HCl, pH 7.6, for 20 min and then in 0.05 M TRIS-HCl, pH 7.6, containing 0.1% BSA
200 for 10 min. Sections were incubated with a secondary goat anti-rabbit antibody conjugated to 10 nm
201 gold particles (British BioCell International, UK), diluted 1:10 in 0.02 M TRIS-HCl buffer, pH 8.2.
202 After rinsing in 0.05 M TRIS-HCl buffer containing 0.1 % BSA for 10 min and in 0.05 M TRIS-
203 HCl buffer for 20 min, the grids were washed three times with distilled water (for 5 min). Sections
204 were subsequently stained with uranyl acetate and lead citrate and observed with a Jeol JEM EX II
205 transmission electron microscope at 100 kV. Pre-immune serum substituted the primary antibody in
206 control sections.

207

208 **2.4 LUV Preparation**

209 LUVs (large unilamellar vesicles) composed, respectively, of 100% POPC (1-palmitoyl-2-oleoyl-
210 sn-glycero-3-phosphocholine) and 70%/30% (w/w) POPC/POPG (POPG 1-palmitoyl-2-oleoyl-sn-
211 glycero-3-phosphoglycerol) were prepared according to general procedures previously reported
212 (Olivieri et al., 2015). Briefly, the lipids dissolved in chloroform were dried under nitrogen flow
213 and then overnight under high vacuum. The lipid film was then hydrated in 1 mL of buffer (20 mM
214 phosphate buffer at pH 7.4 with 150 mM NaCl and 0.8 mM EDTA) and subjected to 5 freeze-thaw
215 cycles. The suspension was extruded through a polycarbonate membrane with an Avanti Polar mini-

216 extruder (20 times through two-stacked polycarbonate membranes with pore sizes of 100 nm) and
217 the obtained LUVs were used within 48 hours of preparation.

218

219 **2.5 Steady state fluorescence experiments**

220 All the steady state fluorescence experiments were performed using a Perkin Elmer LS55 operating
221 at 25 °C in a thermostatic cell holder. The spectra were corrected by subtracting the corresponding
222 blanks.

223 **2.5.1 Outer membrane permeabilization assay**

224 The permeabilization assay was carried-out using the fluorescent probe ANS (1-aminonaphthalene-8-
225 sulfonic acid) as previously described (Domadia et al., 2010; Olivieri et al., 2015; Olivieri et al.,
226 2018). *E. coli* BL21 (DE3) and *Psychrobacter sp.* TAD1 cells were grown, at 37 °C and 15 °C
227 respectively, to mid-log phase in Luria Bertani broth (LB broth from Sigma) were centrifuged,
228 washed and suspended in 10 mM Tris-HCl, 150 mM NaCl, and 0.8 mM EDTA (pH 7.4) buffer to
229 give an OD₆₀₀ of ~1.2. Subsequently, increasing amounts of the Cnd-m3a peptide (from 1.0 to 15.0
230 μM) were added to a quartz cuvette containing 1.0 mL of cell suspension and 5.0 μM ANS.
231 Fluorescence spectra were recorded at wavelengths between 400 and 600 nm with an excitation
232 wavelength of 360 nm. The excitation and emission slit widths were 5 nm. The ANS was
233 incorporated into the membrane and, consequently, the fluorescence intensity increased and blue-
234 shifted.

235 **2.5.2 Partition studies**

236 The ability of peptides to associate with and partition into lipid vesicles was studied by measuring
237 the enhancement of tryptophan fluorescence upon addition of LUVs. Trp-1 fluorescence spectra
238 were recorded at wavelengths between 305 and 500 nm considering an excitation wavelength of
239 295 nm. Measurements were performed with a cross-oriented configuration of polarizers ($Pol_{em}=0^\circ$
240 and $Pol_{exc}=90^\circ$) to reduce contributions from vesicles (Ladokhin et al., 2000). A 1.0 μM peptide
241 solution in 20 mM phosphate buffer at pH 7.4 containing 0.8 mM EDTA and 150 mM NaCl was
242 added to a cuvette and then titrated with LUVs of different compositions (100% POPC and
243 70%/30% POPC/POPG) with a lipid/peptide ratio ranging from 50 to 500 as described previously
244 (Olivieri et al., 2015; Olivieri et al., 2018). The background effects of both buffer and vesicles were
245 subtracted from each spectrum. Mole fraction partition coefficients, K_x , were obtained calculating
246 the fraction of peptide, f_p , which partitioned into the LUVs (Wimley and White, 1993;
247 Rathinakumar and Wimley, 2008; Ladokhin, 2009; Fernández-Vidal et al., 2011). The values of K_x
248 were obtained as described before (Olivieri et al., 2015; Olivieri et al., 2018).

249 **2.5.3 Iodide quenching experiments**

250 Peptide solutions (5.0 μM) in both absence and presence of LUVs (in a peptide:lipid ratio 1:100),
251 were excited at 295 nm and fluorescence spectra were recorded from 305 to 500 nm. The samples
252 were titrated by adding increasing amount of potassium iodide in the range 0.01 - 0.28 M and
253 spectra were recorded with excitation and emission band widths of 2.5 nm. All the fluorescence
254 spectra were corrected for dilution. Fluorescence intensities were extracted and the data were fitted
255 according to the Stern-Volmer equation as described previously (Park et al. 2011; Olivieri et al.,
256 2015; Olivieri et al., 2018).

257

258 **2.6 Negative staining**

259 Samples at the peptide/lipid ratio of 1:100 were prepared with a final lipid concentration of
260 70%/30% (w/w) POPC/POPG vesicles. They were incubated for 10 minutes with 15.0 μM of the
261 Cnd-m3a peptide. Untreated vesicles and lipids at time 0 and 10 min after incubation with the
262 peptide were fixed using 4% PFA in phosphate buffered saline (PBS, Gibco). Droplets of sample
263 suspensions (10 μl) were placed on formvar-carbon coated grids and allowed to adsorb for 60 sec.
264 Excess liquid was removed gently touching the filter paper. The adsorbed specimen was then
265 processed for negative-staining by first washing the specimen grid on a drop of negative stain (2%
266 uranyl acetate in distilled water) and, successively, blotting and repeating this step once more
267 leaving, in this case, the specimen grid for 60 seconds on a new drop of negative stain solution.
268 Samples were observed at a JEOL 1200 EX II electron microscope. Micrographs were acquired
269 with an Olympus SIS VELETA CCD camera equipped the iTEM software.

270

271 **2.7 Hemolytic assay**

272 The hemolytic assay was performed as indicated by Belokoneva et al. (2003). In brief, a 2.5 % (v/v)
273 suspension of human red blood cells from healthy donors in PBS (Gibco) was incubated with serial
274 dilutions of the mutant peptide. Red blood cells were counted by a haemocytometer and adjusted to
275 about 8.0×10^6 cell/ml. Erythrocytes were incubated at 37 °C for 2 h with 10% Triton X-100
276 solution (positive control), PBS (negative control) and with different concentrations of the Cnd-m3a
277 peptide (five dilutions from 50 μM to 0.5 μM , in triplicates). The supernatant was separated from
278 the pellet by centrifugation at 1500x g for 5 min and the absorbance measured at 570 nm. The
279 relative OD compared to that of the positive control defined the percentage of hemolysis. The

280 experiments were performed in triplicate and data shown as mean \pm SD, the statistical analysis was
281 made using the one-way analysis of variance and Bonferroni's post test.

282

283 **2.8 Cell proliferation assay**

284 The peptide Cnd-m3a was dissolved in 100% DMSO (Sigma-Aldrich, USA) to a concentration of
285 10 mM and then diluted and transferred to the bottom of a tissue culture 384 well plate (Greiner
286 Bio One, Austria); the plate was subjected to acoustic droplet ejection (ATS-100, EDC Biosystem,
287 USA) in order to reach the desired final peptide concentration in the culture volume of 40 μ L (the
288 final percentage of DMSO was 0.5%).

289 The cell types reported in Table SI (see Supplementary files) were then plated on compound
290 containing microplates to a density of 2000 cells/well in the final volume of each used medium (40
291 μ L) (see Table SI).

292 After 48 h (72 h for HUVEC only) of incubation at 37 °C and 5% CO₂ in humidified atmosphere,
293 cell proliferation was assessed by CellTiter-Glo following manufacturer's instruction (Promega,
294 USA). Ten different 1:2 dilutions of the peptide Cnd-m3a were tested starting from a concentration
295 of 50 μ M and three independent experiments were performed for each selected concentration. Data
296 analysis was performed by considering four parameter-logistic regression, using GraphPad software
297 (Prism, USA).

298

299 **2.9 Evaluation of Minimal Inhibitory Concentration (MIC) and Minimal Bactericidal 300 Concentration (MBC)**

301 The effects of the Cnd-m3a peptide on microorganism's vitality have been analyzed for Gram – and
302 Gram + positive bacteria. Clinical isolates with assessed resistance profiles were used in this study:
303 *E. coli* ESBL, *Klebsiella pneumoniae* KPC, *Acinetobacter baumannii* XDR, *Pseudomonas*
304 *aeruginosa* MDR, *Staphylococcus aureus* MRSA, *Staphylococcus epidermidis* MRSE and
305 *Enterococcus* spp. VRE. Frozen glycerol stocks were streaked on fresh Trypticase soy agar with 5%
306 sheep blood plate (bioMerieux), incubated at 37° C for 18 h and sub-cultured to produce fresh
307 colonies. A single bacterial colony was used to grow in Mueller-Hinton liquid medium.

308 The CLSI (CLSI, 2015) susceptibility testing protocol was used for the determination of the MICs
309 of the antibacterial agent. The peptide was dissolved in an appropriate buffer and diluted in
310 Mueller-Hinton broth to reach a final concentration of 200 μ g/ mL. Logarithmic phase bacterial
311 cultures were suspended in saline solution to achieve a turbidity equivalent to that of a 0.5
312 McFarland standard and then diluted to a final concentration of 1.2×10^5 CFU/mL. Bacterial

313 suspensions were added to serial dilutions of the peptide (from 0.097 to 100 $\mu\text{g}/\text{mL}$) in a 96-well
314 flat-bottom Microtiter® plate. Both positive (no peptide) and negative (no bacteria) controls were
315 included. The MIC was defined as the lowest compound concentration which prevented visible
316 growth after 24 h of incubation at 37° C. To determine the MBC, aliquots of 100 μL were removed
317 from the wells with no visible microbial growth and plated on Trypticase soy agar plates with 5%
318 sheep blood, than incubated overnight at 37 °C. The MBC was defined as the lowest peptide
319 concentration at which more than 99.9% of the cells were killed compared with an untreated
320 control. All tests were performed in triplicate in two different experimental sessions. A panel of
321 conventional antibiotics have been used as a positive control (see Supplementary files, Table SII).

322

323

324

325

326

327

328

329

330

331

332

333

334

335

336

337

338

339

340

341

342

343

344

345

RESULTS

346

3.1 Peptides design

347 AMPs are short peptides (10-50 amino acids) with an overall positive net charge (usually from +1
348 to +9) and an amount of hydrophobic residues in general close to the 30% of the total molecule.
349 Upon interaction with biological membranes, AMPs fold into amphipathic conformations with the
350 polar residues facing towards the negatively charged head groups of the membrane phospholipids.
351 Starting from the sequence of Cnd (Buonocore et al, 2012), bearing a net charge of +2 at pH 7, we
352 designed a new mutant called Cnd-m3a. Serines 11 and 22, histidines 4, 15, and 17, and, finally,
353 isoleucine 9 have been replaced by lysines (see Figure 1). After the mutation the overall charge is
354 now +8 and the hydrophobic moment 0.564.

355

3.2 Antibody selection

356
357 To detect the interaction of the Cnd-m3a peptide with the bacterial membranes we produced two
358 polyclonal antibodies from rabbits and we selected for the performed experiments the antiserum
359 (named Peps2) showing the best peptide detection in ELISA (see Table I).

360

3.3 Penetration of Cnd-m3a into target bacterial cells

361
362 To evaluate the mechanism of action of Cnd-m3a against bacterial cells, the polyclonal antibody
363 Peps2 has been used and the peptide localization performed by immunoelectron microscopy (Fig.
364 2). The peptide, visualized by gold particles, interact with the target bacterial cells, *Psychrobacter*
365 *sp.*, by electrostatic forces between its positive amino acid residues and the negative exposed
366 charges present on bacterial cell surface. Upon initial investigation at time 0, it was immediately
367 noted that few peptides were closely associated with the bacterial membranes. Cnd-m3a is able to
368 spontaneously traverse *Psychrobacter sp.* outer and inner membranes and, after 10 minutes of
369 incubation, it was found inside the cells, targeting intracellular molecules such as nucleic acids.
370 Once inside the cells, AMPs accumulated in the cytoplasm in a time dependent manner and evident
371 morphological cell damages were induced at 180 minutes, leading to the consequent microbial cell
372 death.

373

3.4 Outer membrane permeabilization assay

374
375 Permeabilization of *E. coli* BL21 (DE3) and *Psychrobacter sp.* TAD1 outer membrane has been
376 studied using the ANS fluorescence. ANS displays a weak fluorescence in aqueous solutions but a
377 very high fluorescence in a hydrophobic environment. Because of its structure, ANS is not able to
378

379 cross the intact outer membrane and thus ANS cannot normally enter in the cell. Upon perturbation
380 or disruption of lipid bilayer, operated by an antimicrobial agent, the ANS can penetrate the cell and
381 its fluorescence emission increases drastically shifting towards lower wavelength (λ). In Figure 3 (A
382 and B) the percentage of ANS uptake for the permeabilization of *E.coli* and *Psychrobacter sp.* upon
383 addition of Cnd and Cnd-m3a is reported. Each experiment has been carried out in triplicate and the
384 standard deviation was $\sim 5\%$. It is evident that the mutant peptide is able to induce a higher
385 perturbation of the bacterial outer membranes compared to the wild type Cnd (see Olivieri et al.,
386 2015). In presence of Cnd-m3a or of Cnd, at a concentration of $1.0 \mu\text{M}$, the percentage of ANS
387 uptake is $\sim 38\%$ and $\sim 21\%$ for *Psychrobacter sp.* and $\sim 56\%$ and $\sim 40\%$ for *E. coli*, respectively.
388 Moreover, at a concentration of $5.0 \mu\text{M}$, Cnd-m3a induces an ANS uptake of $\sim 70\%$ for both *E. coli*
389 and *Psychrobacter sp.*, whereas to obtain the same effect it should occur a $10.0 \mu\text{M}$ and $15.0 \mu\text{M}$
390 concentration of Cnd, respectively. The fluorescence spectra for the permeabilization assay using
391 Cnd-m3a are also reported (C and D).

392

393 **3.5 Partition studies**

394 To study the interaction of peptides with the eukaryotic and prokaryotic membrane we used as
395 membrane models LUVs of different composition. Specifically, a mixture of POPC/POPG (70/30
396 w/w) was used as mimicking system for bacterial membranes and the zwitterionic POPC was used
397 as mimicking system for eukaryotic membranes (Herbig et al., 20005; Reid et al., 2018). The ability
398 of Cnd-m3a to have interaction with and partition into lipid vesicle of different compositions was
399 determined by fluorescence spectroscopy of Trp-1 for each peptide. Tryptophan fluorescence is
400 commonly used to determine the polarity of the local environment. Specifically, as the polarity of
401 the environment decreases the Trp fluorescence shifts to a lower wavelength (blue shift) and
402 increases its intensity. The shift and the enhancement in the fluorescence emission spectrum (Figure
403 4) suggest that the Cnd-m3a peptide is able to interact and bind to the lipid vesicles of different
404 composition, 100% POPC and 70%/30% POPC/POPG. LUVs entirely composed of POPC, a
405 zwitterionic lipid with no net charge, were used to mimic mammalian cell membranes, whereas
406 LUVs containing also POPG, a lipid head group bearing a net negative charge, were chosen to
407 mimic the net anionic surface charge of bacterial membrane. To evaluate the mole fraction partition
408 coefficients K_x , we plotted the binding isotherms derived from the titration of peptides (Figure 4).
409 The values of K_x have been determined and reported in Table II with the selectivity ratio defined as
410 the ratio between the partition coefficient determined for 70%/30% POPC/POPG and the one for
411 100% POPC. Partitioning data suggest that Cnd-m3a has weaker interactions with LUVs composed

412 exclusively of POPC ($K_x = (5.1 \pm 0.2) \times 10^4$), thus showing a higher affinity and selectivity towards
413 POPC/POPG LUVs ($K_x = (25.0 \pm 0.9) \times 10^4$), which mimics the prokaryotic cell membranes.
414 Noteworthy, is the high value of the selectivity ratio, ~ 5 , indicating its higher preference for
415 vesicles mimicking the bacterial cell membrane if compared to the wild type Cnd (see Olivieri et
416 al., 2015).

417

418 **3.6 Iodide quenching**

419 Successively, the accessibility of tryptophan to the iodide dynamic quencher was investigated and
420 in Figure 5 the Stern-Volmer plots in absence and presence of lipid vesicles are reported for both
421 Cnd (Olivieri et al., 2015) and Cnd-m3a. Stern-Volmer plots for peptides fit linearly, indicating a
422 collision mechanism of quenching, and the corresponding K_{SV} (Stern-Volmer constants) determined
423 values are reported in Table III. The Trp-1 showed high solvent accessibility for both peptides in
424 buffer and high values of K_{SV} have been determined (10.4 and 8.3 M^{-1} , for Cnd and Cnd-m3a,
425 respectively). The smaller values of K_{SV} obtained in presence of LUVs, clearly indicate a great
426 solvent protection of Trp-1 due to a strong interaction with the bilayer lipid environment. The
427 similar trend observed (Figure 5) for the wild type and the mutant peptides in presence of lipid
428 vesicles of different composition suggest that both interact with the LUVs and that the Trp-1 is not
429 solvent-exposed.

430 The net accessibility factors (NAF) were defined by the formula:

$$431 \text{ NAF} = \frac{(K_{SV})_{LUV}}{(K_{SV})_{buffer}}$$

432 as the ratio between the Stern-Volmer constant in presence and in absence of LUV (Saikia et al.,
433 2018). The small values of NAF suggest that the Trp residue is largely inaccessible to the quencher,
434 due to a strong interaction with the lipid bilayer. In presence of 100% POPC vesicles, the membrane
435 mimicking system for eukaryotic cells, the values of NAF are nearly the same for both peptides.
436 However, in presence of 70%/30% POPC/POPG vesicles, the Cnd-m3a peptide shows a smaller
437 value of NAF, 0.18, with respect to 0.24 for Cnd, thus indicating an improved preference for
438 anionic lipid vesicles.

439

440 **3.7 Effect of Cnd-m3a on POPC/POPG LUVs**

441 TEM analysis (Figure 6) showed that the Cnd-m3a peptide alters the 70%/30% POPC/POPG
442 LUVs membranes, leading to the formation of roughening and surface ruptures if compared to the
443 smooth membranes found in untreated vesicles. Moreover, Cnd-m3a peptide induced, after 10

444 minutes of incubation, membrane curvature and change in the POPC/POPG LUVs shape, which is
445 evident by the largely found non spherical LUVs compared with the nearly spherical shape with
446 round edges present in the untreated ones.

447

448 **3.8 Hemolytic and cytotoxicity assays on Cnd-m3a**

449 The hemolytic effect of the Cnd-m3a peptide has been tested on human erythrocytes to investigate
450 its capacity to induce membrane lysis. Five concentrations have been used (starting from a
451 concentration of 50 μ M with successive dilutions) that correspond for the first point to about 120 μ g
452 of peptide (Figure 7). The percentage of hemolysis is quite low at 3 μ M (about 5 %) and it reaches
453 the maximum (about 30 %) at the highest tested concentration value (50 μ M). All differences were
454 statistically significant compared to the lowest tested peptide concentration (3 μ M).

455 The cytotoxicity of the Cnd-m3a peptide was investigated, in a dose response manner starting from
456 50 μ M and performing ten 1:2 successive dilutions, on one primary human endothelial cell line
457 (HUVEC) and on a panel of cancer cell lines for the determination of its anti-proliferative potential.
458 No inhibition of cell proliferation was appreciable at all tested concentrations both in the case of
459 normal as in tumoral cell lines (Table IV).

460

461 **3.9 Antibacterial activity of Cnd-m3a**

462 *In vitro* experiments were conducted to investigate the antibacterial activity of Cnd-m3a. A total of
463 7 clinical isolates belonging to clinically-relevant multidrug-resistant bacteria were tested. Strains
464 were previously identified by standard morphological, cultural and biochemical tests. The MICs and
465 MBCs values are summarized in Table V. The obtained data showed that the peptide exerted the
466 strongest bactericidal activity on Gram – bacteria, as expected by the high affinity of this molecule
467 towards their cell membrane and evidenced by the results of the previously reported partition and
468 iodide quenching studies. Conventional antibiotics have been used as positive controls of the tested
469 bacterial strains resistance (see supplementary files Table II).

470

471

472

473

474

475

476

DISCUSSION

477

478

479

480

481

482

483

484

485

486

487

488

489

490

491

492

493

494

495

496

497

498

499

500

501

502

503

504

505

506

507

508

During last years the antibiotic resistance, the ability of bacteria to withstand to the effects of usual medications, is highly increasing and it is now a serious global public health threat. According to the Centers for Disease Control and Prevention (CDC), 2 million people in the U.S. develop antibiotic-resistant infections each year, and at least 23.000 people die from those infections (<https://www.cdc.gov/drugresistance/>). Intensive research is therefore directed towards the identification of new and non-conventional anti-infective molecules, and AMPs have been considered as possible candidates. They have been identified in all living organisms showing also immunomodulatory properties, which make them the compounds most intensively studied for the development of novel therapeutics in this field (Mahlapu et al., 2016).

A high number of AMPs, starting from the first peptide isolated from the skin of the winter flounder in 1997 (Cole et al., 1997), have been isolated from fish that, living in an aquatic environment with a high microbial load, have evolved a potent innate immune system (Rakers et al., 2013; Shabir et al., 2018). Thus, we decided some years ago to investigate the presence of AMPs in a teleost, the *Chionodraco hamatus* (Perciformes: Channichthyidae), adapted to resist in an extreme environment like the Antarctica, as this species was considered a model for its adaptations to subzero temperatures that involved peculiar physiological features (Ruud, 1954; Bargelloni et al., 1994). The isolated peptide was named chionodracine (Cnd), and its molecular characterization and bactericidal activity was firstly investigated (Buonocore et al., 2012). The peptide showed all the expected features of a fish AMP and it was biologically active against endemic bacteria from Antarctica (*Psychrobacter* sp. TAD1 and *Psychrobacter* sp. TAD144). Unfortunately, although it showed low hemolytic effect, it was not active against human bacterial pathogens as another Antarctic AMP recently identified (Shin et al., 2017). Successively, we studied its structure, its interaction with different membranes and we determined that it adopts a canonical α -helical structure upon the interaction with lipid membranes, with a preference towards negatively charged lipids and *E. coli* extracts (Olivieri et al., 2015). Taking into account our previous results, starting from the Cnd template, we designed a new mutant peptide with the aim to obtain a molecule more active against human bacterial pathogens. Therefore, we introduced in this new sequence, named Cnd-m3a, more positive charged amino acids (the total net positive charge is now +8), as this aspect is crucial for the interaction with the negatively charged membranes of bacteria, and, moreover, we disrupted the amphipathicity of the nonpolar face to improve the antimicrobial activity by increasing the specificity and selectivity towards bacterial membranes and decreasing the cytotoxicity towards mammalian membranes (Chen et al., 2005). A similar strategy was used in the

509 designing of other three mutants, KS-Cnd, KH-Cnd and KHS-Cnd, but with a maximum total net
510 charge of +7, in KSH-Cnd, and preserving the original α -helix conformation (Olivieri et al, 2018).

511 Using a polyclonal antibody rose against Cnd-m3a we demonstrated by immunoelectron
512 microscopy that the peptide absorbs on the membrane surface of the bacteria *Psychrobacter* sp.
513 TAD1 and, after entering inside the cell it targets the DNA causing cell death. Very recently, He
514 and colleagues identified an antimicrobial peptide from red drum (*Sciaenops ocellatus*) (He et al.,
515 2018) and demonstrated *in vitro* that it was able to induce degradation of bacterial nucleic acids
516 (both DNA and RNA). However, this is the first time, on our knowledge, that this kind of
517 mechanisms has been demonstrated in *in vivo* studies, by immunoelectron microscopy on target
518 bacteria, for a fish AMP. Successively, we investigated the interaction of the Cnd-m3a peptide with
519 two different synthetic unilamellar vesicles, one formed only of POPC (1-palmitoyl-2-oleoyl-sn-
520 glycerol-3-phosphocholine), which mimics mammalian membranes that are composed of
521 zwitterionic lipids with no net charge (Zaslhoff, 2002), and the other composed of 70% POPC and
522 30% POPG (1-palmitoyl-2-oleoyl-sn-glycerol-3-phosphoglycerol), which is more similar to
523 bacterial membranes as POPG is negatively charged (Yeaman and Yount, 2003). Both outer
524 membrane permeabilisation assay and partition studies evidenced that the mutant peptide acts
525 preferentially against POPC/POPG vesicles with a higher activity compared to the wild type Cnd
526 and also with a higher selectivity ratio compared to the other three mutants previously designed
527 (Olivieri et al., 2018). The action on synthetic membranes of piscidin 1 has been simulated in a
528 recent paper and the obtained results evidenced that the membrane disruption was not due to the
529 formation of stable pores but, rather than, to the formation of transitory distortions of the
530 bilayer/water interface (Perrin et al., 2016): this results is in agreement with the mechanism of
531 bacteria degradation we demonstrated for Cnd-m3a and with its effects on POPC/POPG LUVs we
532 determined by TEM-analysis.

533 To evaluate the possible use of the Cnd-m3a peptide as a new therapeutic drug, we studied
534 its hemolytic activity against human erythrocytes and it resulted of about 5 % at the lowest tested
535 concentration (3 μ M), a slightly higher value if compared to the same data obtained for both Cnd
536 and the three mutants (Olivieri et al., 2015; Olivieri et al., 2018). We investigated also the cytotoxic
537 effect of the Cnd-m3a mutant against a primary human endothelial cell line (HUVEC) with no
538 evident effect at all tested concentrations (the maximum was 50 μ M). Therefore the peptide should
539 have no or very low effects on normal mammalian cells, as it was expected.

540 We further investigated the potentiality of the peptide studying its antibacterial activity
541 against multidrug resistant human pathogens. The results were very interesting as the Cnd-m3a was

542 active, with MIC values around 5-10 μM , especially against Gram – bacteria. This bacteria, in
543 contrast to Gram + positive bacteria where cytoplasmic membrane is surrounded by a thick
544 peptidoglycan layer, present a cytoplasmic membrane surrounded by a thin peptidoglycan layer as
545 well as an outer membrane (Lin and Weibel, 2016). The MBC and MIC values are very similar to
546 the ones obtained for the other three Cnd mutants on the same tested bacteria (Olivieri et al., 2018)
547 and lower than the MIC values presented in a recent paper (Jiang et al., 2014) for piscidin-1 against
548 *Pseudomonas aeruginosa*. It has also to be considered that, at a peptide concentration of 5-10 μM
549 we detected a low effect of Cnd-m3a on mammalian cells, as described before. Finally, we
550 determined the Therapeutic Index (TI) for the peptide (data not shown), a widely accepted
551 parameter to represent the specificity of antimicrobial peptides for prokaryotic *versus* eukaryotic
552 cells (Jiang et al., 2014) that is calculated by the ratio of HC_{50} (50% of hemolytic activity) and MIC,
553 in relation to Gram – bacteria, and we obtained values in accordance to the results obtained for the
554 other studied three Cnd mutants (Olivieri et al., 2018)

555 In conclusion, our data makes the Cnd-m3a peptide an excellent candidate for the
556 development of a possible new antimicrobial agent. However, the further addition of a positive net
557 charge have not dramatically increased the antimicrobial activity of this new mutant compared to
558 the other three already designed. Future studies will be addressed to investigate, *in vivo* on animal
559 models, the toxicity, the pharmacokinetics and the pharmacodynamics of the Cnd-m3a peptide to
560 finally address its use on clinical trials.

561
562
563
564
565
566
567
568
569
570
571
572
573
574

575

ACKNOWLEDGEMENTS

576 This work was partially funded by the PRONAT project supported by CNCCS s.c.s.r.l..

577

578

REFERENCES

579

580 Bargelloni, L., Ritchie, P.A., Patarnello, T., Battaglia, B., Lambert, D.M., Meyer, A., 1994.
581 Molecular evolution at subzero temperatures: mitochondrial and nuclear phylogenies of fishes from
582 Antarctica (suborder Notothenioidei), and the evolution of antifreeze glycopeptides. *Mol. Biol.*
583 *Evol.* 11, 854-863.

584

585 Belokoneva, O.S., Villegas, E., Corzo, G., Dai, L., Nakajima, T., 2003. The hemolytic activity of six
586 arachnid cationic peptides is affected by the phosphatidylcholine-to-sphingomyelin ratio in lipid
587 bilayers. *Biochim. Biophys. Acta* 1617, 22-30.

588

589 Bulet, P., Stocklin, R., Menin, L., 2004 Anti-microbial peptides: from invertebrates to vertebrates.
590 *Immunol. Rev.* 198, 169-184.

591

592 Buonocore, F., Randelli, E., Casani, D., Picchiatti, S., Belardinelli, M.C., de Pascale, D., De Santi,
593 C., Scapigliati, G., 2012. A piscidin-like antimicrobial peptide from the icefish *Chionodraco*
594 *hamatus* (Perciformes: Channichthyidae) molecular characterization, localization and bactericidal
595 activity, *Fish Shellfish Immunol.* 33, 1183–1191.

596

597 Campagna, S., Saint, N., Molle, G., Aumelas, A., 2007. Structure and mechanism of action of the
598 antimicrobial peptide piscidin. *Biochemistry* 46, 1771–1778.

599

600 Chen, Y., Mant, C.T., Farmer, S.W., Hancock, R.E., Vasil, M.L., Hodges, R.E., 2005. Rational
601 design of alpha-helical antimicrobial peptides with enhanced activities and specificity/therapeutic
602 index. *J. Biol. Chem.* 280, 12316-12329.

603

604 Chia, T.J., Wu, Y.C., Chen, J.Y., 2010. Antimicrobial peptides (AMP) with antiviral activity
605 against fish nodavirus. *Fish. Shellfish Immunol.* 28, 434–439.

606

607 CLSI. Performance Standards for Antimicrobial Susceptibility Testing. Vol. 25 Informational
608 Supplement. Wayne, PA: Clinical Laboratory Standards Institute, 2015: M100-S25.

609

610 Cole, A.M., Weis, P., Diamond, G., 1997. Isolation and characterization of pleurocidin, an
611 antimicrobial peptide in the skin secretions of winter flounder, *J. Biol. Chem.* 272, 12008–12013.

612

613 Colorni, A., Ullal, A., Heinisch, G., Noga, E.J., 2008. Activity of the antimicrobial polypeptide
614 piscidin 2 against fish ectoparasites. *J. Fish. Dis.* 31, 423–432.

615

616 Corrales, J., Gordon, W.L., Noga, E.J., 2009. Development of an ELISA for quantification of the
617 antimicrobial peptide piscidin 4 and its application to assess stress in fish. *Fish Shellfish Immunol.*
618 27, 154–163.

619

620 Domadia, P.N., Bhunia, A., Ramamoorthy, A., Bhattacharjya, S., 2010. Structure, interactions, and
621 antibacterial activities of MSI-594 derived mutant peptide MSI-594F5A in lipopolysaccharide
622 micelles: role of the helical hairpin conformation in outer membrane permeabilization. *J. Am. Chem.*
623 *Soc.* 132, 18417–18428.

- 624
625 Fernández-Vidal, M., White, S.H., Ladokhin, A.S., 2011. Membrane partitioning: “classical” and
626 “nonclassical” hydrophobic effects. *J. Membr. Biol.* 239, 5–14.
627
- 628 Hancock, R.E.W., Lehrer, R., 1998. Cationic peptides: a new source of antibiotics, *Trends*
629 *Biotechnol.* 16, 82–88.
630
- 631 He, S.-w., Wang, G.-h., Yue, B., Zhou, S., Zhang, M., 2018. TO17: A teleost antimicrobial peptide
632 that induces degradation of bacterial nucleic acids and inhibits bacterial infection in red drum,
633 *Sciaenops ocellatus*. *Fish Shellfish Immunol.* 72, 639-645.
634
- 635 Herbig, M.E., Fromm, U., Leuenberger, J., Krauss, U., Beck-Sickinger, A.G., Merkle, H.P., 2005.
636 Bilayer interaction and localization of cell penetrating peptides with model membranes: a
637 comparative study of a human calcitonin (hCT)-derived peptide with pVEC and pAntp(43-58).
638 *Biochim. Biophys. Acta* 1712, 197-211.
639
- 640 Hilchie, A.L., Doucette, C.D., Pinto, D.M., Patrzykat, A., Douglas, S., Hoskin, D.W., 2011.
641 Pleurocidin-family cationic antimicrobial peptides are cytolytic for breast carcinoma cells and
642 prevent growth of tumor xenografts. *Breast Cancer Res.* 13, R102.
643
- 644 Hsu, J.C., Lin, L.C., Tzen, J.T., Chen, J.Y., 2011. Characteristics of the antitumor activities in
645 tumor cells and modulation of the inflammatory response in RAW264.7 cells of a novel
646 antimicrobial peptide, chrysophsin-1, from the red sea bream (*Chrysophrys major*). *Peptides* 32
647 (2011) 900–910.
648
- 649 Jiang, Z., Vasil, A.I., Vasil, M.L., Hodges, R.S., 2014. “Specificity determinants” improve
650 therapeutic indices of two antimicrobial peptides piscidin 1 and dermaseptin S4 against the Gram-
651 negative pathogens *Acinetobacter baumannii* and *Pseudomonas aeruginosa*. *Pharmaceutics* 7,
652 366-291.
653
- 654 Ladokhin, A.S., Jayasinghe, S., White, S.H., 2000. How to measure and analyze tryptophan
655 fluorescence in membranes properly, and why bother? *Anal. Biochem.* 285, 235–245.
656
- 657 Ladokhin, A.S., 2009. Fluorescence spectroscopy in thermodynamic and kinetic analysis of pH-
658 dependent membrane protein insertion. *Methods Enzymol.* 466, 19–42.
659
- 660 Lin, T.Y., Weibel, D.B. 2016. Organization and function of anionic phospholipids in bacteria. *Appl.*
661 *Microbiol. Biotechnol.* 100, 4255–4267.
662
- 663 Mahlapuu, M, Hakansson J., Ringstad L., Bjorn C., 2016. Antimicrobial peptides: an emerging
664 category of therapeutic agents. *Front. Cell. Infect. Microbiol.* 6: 194.
665
- 666 Mulero, I., Noga, E.J., Meseguer, J., Garcia-Ayala, A., Mulero, V., 2008. The antimicrobial
667 peptides piscidins are stored in the granules of professional phagocytic granulocytes of fish and are
668 delivered to the bacteria-containing phagosome upon phagocytosis. *Dev. Comp. Immunol.* 32,
669 1531–1538.
670
- 671 Noga, E.J., Silphaduang, U., 2003. Piscidins: a novel family of peptide antibiotics from fish. *Drug*
672 *News Perspect.* 16, 87–92.

673

674 Olivieri, C., Buonocore, F., Picchietti, S., Taddei, A.R., Scapigliati, G., Dicke, A.A., Vostrikov,
675 V.V., Bernini, C., Veglia, G., Porcelli, F., 2015. Structure and membrane interactions of
676 chionodracine, a piscidin-like antimicrobial peptide from the icefish *Chionodraco hamatus*.
677 *Biochim. Biophys. Acta* 1848, 1285-1293.

678

679 Olivieri, C., Bugli, F., Menchinelli, G., Veglia, G., Buonocore, F., Scapigliati, G., Stocchi, V.,
680 Ceccacci, F., Papi, M., Sanguinetti, M., Porcelli, F., 2018. Design and characterization of
681 chionodracine-derived antimicrobial peptides with enhanced activity against drug-resistant human
682 pathogens. *RSC Adv.* 8, 41331-41346.

683

684 Pan, C.Y., Chen, J.Y., Cheng, Y.S.E., Chen, C.Y., Ni, I.H., 2007. Gene expression and localization
685 of the epinecidin-1 antimicrobial peptide in the grouper (*Epinephelus coiodes*), and its role in
686 protecting fish against pathogenic infection. *DNA Cell. Biol.* 26, 403–413.

687

688 Park, N.G., Silphaduang, U., Moon, H.S., Seo, J.K., Corrales, J., Noga, E.J., 2011. Structure-
689 activity relationships of piscidin 4, a piscine antimicrobial peptide, *Biochemistry* 50, 3288–3299.

690

691 Perrin, B.S.Jr., Fu, R., Cotten, M.L., Pastor R.W., 2016. Simulations of membrane-disrupting
692 peptides II: AMP piscidin 1 favors surface defects over pores. *Biophys. J.* 111, 1258-1266.

693

694 Rajanbabu, V., Chen, J.-Y., 2011. Applications of antimicrobial peptides from fish and perspectives
695 for the future. *Peptides* 32, 415-420.

696

697 Rakers, S. Niklasson, L., Steinhagen, D., Kruse, C., Schaubert, J., Sundell, K., Paus, R., 2013.
698 Antimicrobial peptides (AMPs) from fish epidermis: perspectives for investigative dermatology. *J.*
699 *Invest. Dermatol.* 133, 1140-1149.

700

701 Rathinakumar, R., Wimley, W.C., 2008. Biomolecular engineering by combinatorial design and
702 high-throughput screening: small, soluble peptides that permeabilize membranes. *J. Am. Chem.*
703 *Soc.* 130, 9849–9858.

704

705 Ravichandran, S., Kumaravel, K., Rameshkumar, G., AjithKumar T.T., 2010. Antimicrobial
706 peptides from the marine fishes. *Res. J. Immunol.* 3, 146-156.

707

708 Reid, K.A., Davis, C.M., Dyer, R.B., Kindt, J.T., 2018. Binding and insertion of a β -hairpin peptide
709 at a lipid bilayer surface: influence of electrostatics and lipid tail packing. *Biochim. Biophys. Acta*
710 *Biomembr.* 1860: 792-800.

711

712 Ruud, J.T., 1954. Vertebrates without erythrocytes and blood pigment. *Nature* 173, 848-850.

713

714 Saikia, K., Chaudary, N., 2018 Interaction of MreB-derived antimicrobial peptides with
715 membranes. *Biochem. Biophys. Res. Comm.* 498, 58-63.

716

717 Shabir, U., Ali, S., Magray A.R., Ganai B.A., Firdous P., Hassan T., Nazir R., 2018. Fish
718 antimicrobial peptides (AMP's) as essential and promising molecular therapeutic agents: A review.
719 *Microb. Pathog.* 114, 50-56.

720

- 721 Shi, J., Camus, A.C., 2006. Hecpidin in amphibian and fishes: antimicrobial peptides or iron
722 regulatory hormones, *Dev. Comp. Immunol.* 30, 746–755.
723
- 724 Shin, S.C., Ahn, I.H., Ahn, D.H., Lee, Y.M., Lee, J.H., Kim, H.-W., Park, H., 2017.
725 Characterization of two antimicrobial peptides from Antarctic fishes (*Notothenia coriiceps* and
726 *Parachaenichthys charcoti*). *PLoS ONE*, 12(1): e0170821.
727
- 728 White, S.H., Wimley, W.C., 1998 Hydrophobic interactions of peptides with membrane interfaces,
729 *Biochim. Biophys. Acta* 1376, 339-352.
730
- 731 Wimley, W.C., White, S.H., 1993. Membrane partitioning: distinguishing bilayer effects from the
732 hydrophobic effect. *Biochemistry* 32, 6307–6312.
733
- 734 Yeaman, M.R., Yount, N.Y. 2003. Mechanisms of antimicrobial peptide action and resistance.
735 *Pharmacol.Rev.* 55, 27–55.
736
- 737 Zasloff, M., 2002. Antimicrobial peptides of multicellular organisms. *Nature* 415, 389-95.
738
- 739 Zavascki, A.P., Goldani, L.Z., Li, J., Nation, R.L., 2007. Polymyxin B for the treatment of
740 multidrug-resistant pathogens: a critical review. *J. Antimicrob. Chemother.* 60, 1206–1215.
741
742
743
744
745
746
747
748
749
750
751
752
753
754

755

756

757

758

759

760

761

762

763

FIGURE LEGENDS

764 **Figure 1.** Alignment of the wild type peptide (Cnd) and the mutant (Cnd-m3a). The positively
765 changed amino acids have been evidenced in bold for Cnd and in bold and underlined for Cnd-m3a.
766 The conserved amino acids are indicated with an “*” below the sequences, while “.” and “:” show
767 amino acids with conserved physical and/or chemical properties.

768

769 **Figure 2.** Representative TEM immunogold images of *Psychrobacter* sp. cells incubated with Cnd-
770 m3a. (A, B, C) Bacteria incubated with Cnd-m3a peptide for 0, 10 and 180 minutes, respectively.
771 (D) Untreated bacteria. The peptide first interacts with the membranes and once inside the cells
772 preferentially targets the DNA. The black arrows in panel (G) indicate cytoplasm disruptions. Bars:
773 from A to H = 500 nm.

774

775 **Figure 3.** Percentage of permeabilization for *E. coli* (A) and *Psychrobacter* sp. (B) outer
776 membranes obtained using Cnd or Cnd-m3a. The experiments were performed in triplicate and an
777 illustrative result is showed. Fluorescence spectra for the permeabilization assay using Cnd-m3a are
778 also reported (C and D).

779

780 **Figure 4.** Binding isotherm (25 °C) for Cnd-m3a interacting with LUVs with different lipid compositions.
781 The fluorescence of tryptophan was measured; lipid vesicles were added to samples containing 1.0 μM
782 peptide.

783

784 **Figure 5.** Stern-Volmer plot showing the Trp-1quenching by KI for Cnd and Cnd-m3a. The
785 experiments were performed in quadruplicate and representative results are shown.

786

787 **Figure 6. Negative staining of 70%/30% POPC/POPG LUVs.** (A) Untreated LUVs and (B) higher
788 magnification showing the smooth membranes. (C) Vesicles incubated with Cnd-m3a peptide at
789 time 0 and (D) higher magnification membrane roughening (arrow heads). (E) Cnd-m3a-treated
790 LUVs after 10 minutes of incubation and (F) higher magnification showing membrane curvature
791 and change in the vesicles shape (arrows). Bars: A, C and E 500 nm; B, D and F 200 nm.

792

793 **Figure 7.** Hemolytic activity of the Cnd-m3a peptide against human erythrocytes. Five different
794 concentrations have been tested, starting from 50 μM with successive dilutions. The values
795 represent the mean ± SD (n=3). A positive control was determined using 10% Triton X-100
796 solution and it was considered as 100% of hemolysis. **= p < 0.01 with respect to the 3 μM; ***=
797 p < 0.001 with respect to 3 μM; N=3.

798

799

800

801

802

803

804

805

806

807

808

809

810

TABLE LEGENDS

811
812
813
814
815
816
817
818
819
820
821
822
823
824
825
826
827
828
829

Table I. ELISA assay to define the best antiserum against Cnd-m3a. Optical density values (OD at 450 nm) are the mean absorbance \pm SD of triplicate wells at different dilutions of the antisera.

Table II. Partition parameters for the mutant and the wild type peptide in the presence of 100 % POPC or 70%/30% POPC/POPG.

Table III. Stern–Volmer quenching constants (K_{SV}) and NAF values obtained for the two peptides in the presence of different lipid vesicles. The peptide/lipid molar ratio was 1:100 in all performed experiments.

Table IV. Cytotoxicity assays results for all tested cell lines. The data are presented as the mean \pm SD of three independent experiments.

Table V. *In vitro* susceptibility of 70 clinical isolates of *E. coli*, *K. pneumoniae*, *A. baumannii*, *P. aeruginosa*, *S. aureus*, *S. epidermidis* and *Enterococcus* spp with known resistance profiles to Cnd-m3a. The reported MICs and MBCs are the average values \pm SD from 10 isolate experiments for each species. The range of the obtained values is also presented.

Table I.

Peps1		Cnd-m3a
	Dil. 1:10	0.202±0.020
	Dil. 1:100	0.060±0.008
	Dil. 1:1000	0.043±0.005
	Dil. 1:5000	0.030±0.003

Peps2		Cnd-m3a
	Dil. 1:10	1.328±0.045
	Dil. 1:100	0.899±0.040
	Dil. 1:1000	0.656±0.020
	Dil. 1:5000	0.131±0.012

Table II.

<i>Peptide</i>	<i>Lipid Mixture</i>	$K_x (x10^4)$	<i>Selectivity ratio</i>
Cnd	100% POPC	3.43 ± 0.26	1.43
	70%/30% POPC/POPG	4.91 ± 0.29	
Cnd-m3a	100% POPC	5.1 ± 0.2	4.90
	70%/30% POPC/POPG	25.0 ± 0.9	

Table III.

	100% POPC		70%/30% POPC/POPG		Buffer	
	$K_{SV} (M^{-1})$	NAF	$K_{SV} (M^{-1})$	NAF	$K_{SV} (M^{-1})$	NAF
Cnd	2.9 ± 0.1	0.28	2.5 ± 0.1	0.24	10.4 ± 0.3	1
Cnd-m3a	2.5 ± 0.1	0.30	1.5 ± 0.1	0.18	8.3 ± 0.3	1

Table IV.

Conc (nM)	HUVEC prol. (72h inc)		OVCAR5 prol. (48h inc)		A549 prol. (48h inc)		K562 prol. (48h inc)		HUH7 prol. (48h inc)		HeLa prol. (48h inc)		PC3 prol. (48h inc)		SH-SY5Y prol. (48h inc)	
	% viable cells	SD	% viable cells	SD	% viable cells	SD	% viable cells	SD	% viable cells	SD	% viable cells	SD	% viable cells	SD	% viable cells	SD
64000	96,15537	3,8446	100,3706	0,3706	105,3556	5,3556	90,90531	9,0947	92,05963	7,9404	101,8847	1,8847	95,60587	4,3941	106,2453	6,2453
32000	88,75033	11,25	103,1796	3,1796	88,62649	11,374	102,6698	2,6698	95,29737	4,7026	100,6868	0,6868	105,5163	5,5163	100,1379	0,1379
16000	104,533	4,533	93,1307	6,8693	92,07398	7,926	105,933	5,933	106,4775	6,4775	88,80672	11,193	90,63387	9,3661	103,5688	3,5688
8000	95,71216	4,2878	102,1754	2,1754	92,77121	7,2288	88,61385	11,386	109,426	9,426	106,1609	6,1609	94,51285	5,4871	106,8167	6,8167
4000	112,0595	12,06	104,69	4,69	88,34805	11,652	93,59661	6,4034	89,82394	10,176	112,2077	12,208	91,29074	8,7093	105,1012	5,1012
2000	101,9691	1,9691	92,78011	7,2199	99,81451	0,1855	93,0051	6,9949	91,33071	8,6693	103,7148	3,7148	92,56275	7,4372	88,80294	11,197
1000	104,956	4,956	107,3523	7,3523	110,9368	10,937	109,4318	9,4318	105,2652	5,2652	101,9829	1,9829	102,8112	2,8112	106,3035	6,3035
500	92,94393	7,0561	111,4265	11,427	97,39573	2,6043	91,89226	8,1077	88,38365	11,616	104,5596	4,5596	96,5681	3,4319	90,73578	9,2642
250	94,46924	5,5308	99,74733	0,2527	110,712	10,712	99,74444	0,2556	94,40342	5,5966	104,2904	4,2904	100,8805	0,8805	101,877	1,877
125	94,47279	5,5272	96,40509	3,5949	102,6199	2,6199	97,08855	2,9114	100,1267	0,1267	110,7138	10,714	101,9513	1,9513	111,3053	11,305

Table V.

Bacterial Strains	MIC ($\mu\text{g}/\text{mL}$)		MBC ($\mu\text{g}/\text{mL}$)	
	Median \pm SD	Range	Median \pm SD	Range
Gram – bacteria				
<i>E. coli</i> ESBL	6.25 \pm 0.0	6.25-6.25	25 \pm 0.0	25-25
<i>K. pneumoniae</i> KPC	12.5 \pm 5.1	12.5-25	25 \pm 0.0	25-25
<i>A. baumannii</i> XDR	6.25 \pm 3.1	3.12-6.25	12.5 \pm 6.5	12.5-25
<i>P. aeruginosa</i> MDR	12.5 \pm 0.0	12.5-12.5	25 \pm 0.0	25-25
Gram + bacteria				
<i>S. aureus</i> MRSA	25 \pm 10.2	25-50	50 \pm 0.0	50-50
<i>S. epidermidis</i> MRSE	25 \pm 0.0	25-25	50 \pm 10.2	25-50
<i>Enterococcus</i> spp. VRE	25 \pm 10.2	25-50	50 \pm 0.0	50-50

Figure 1**A**

Cnd-m3a

WFGKLYRGKTKVVKKVKGLLKG

Cnd

FFGHLYRGITSVVKHVHGLLSG

:***:**** * .***:***:***.*

ACCEPTED MANUSCRIPT

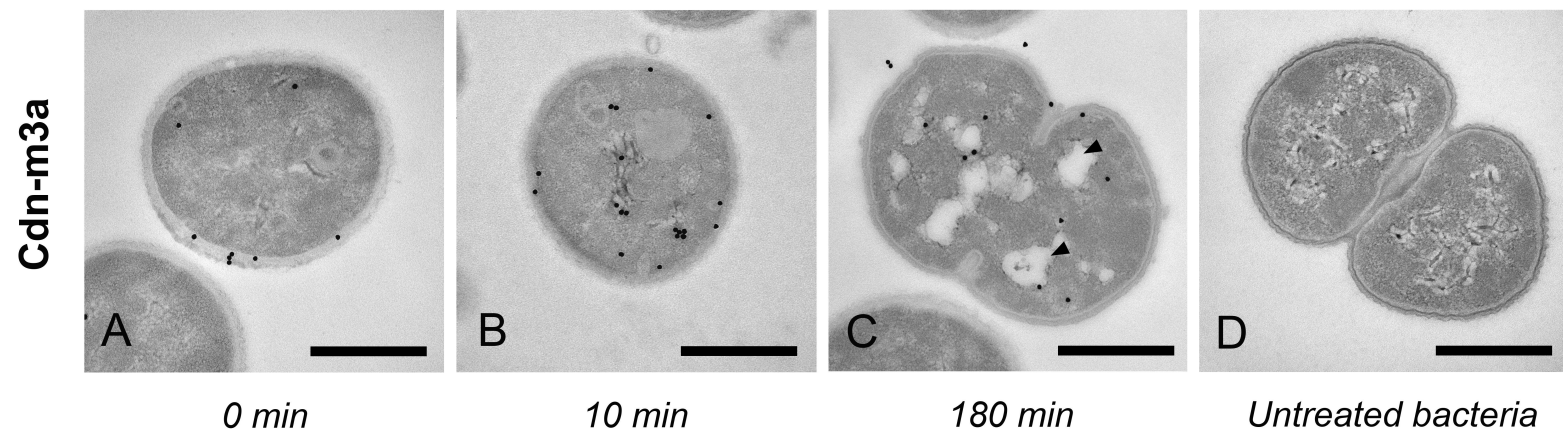


Figure 2

Figure 3.

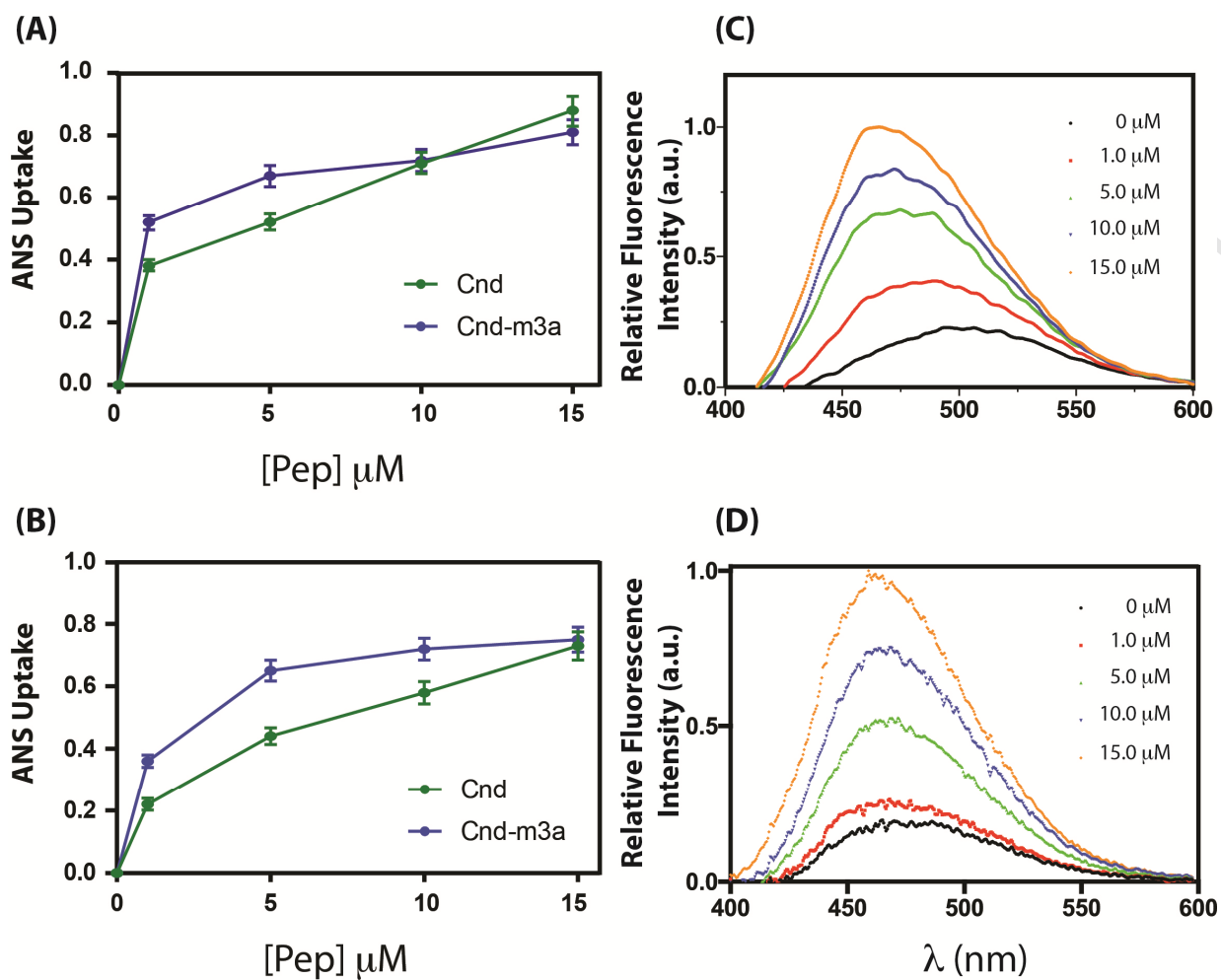


Figure 4.

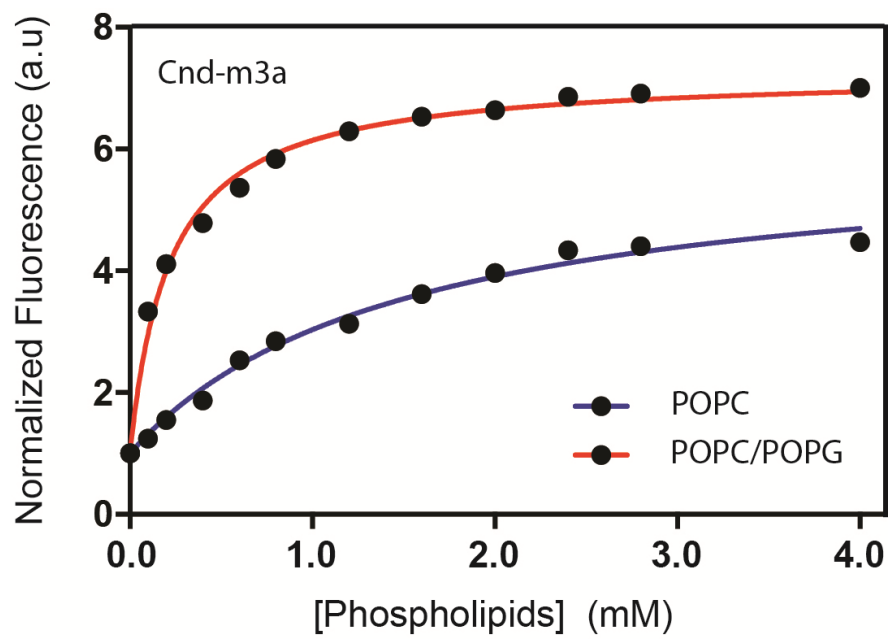
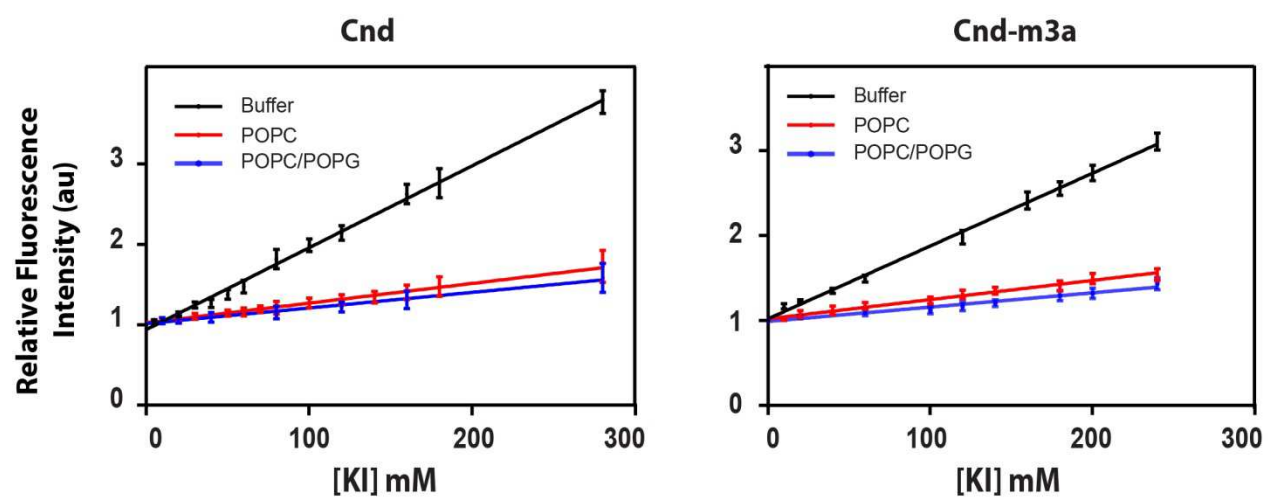


Figure 5.



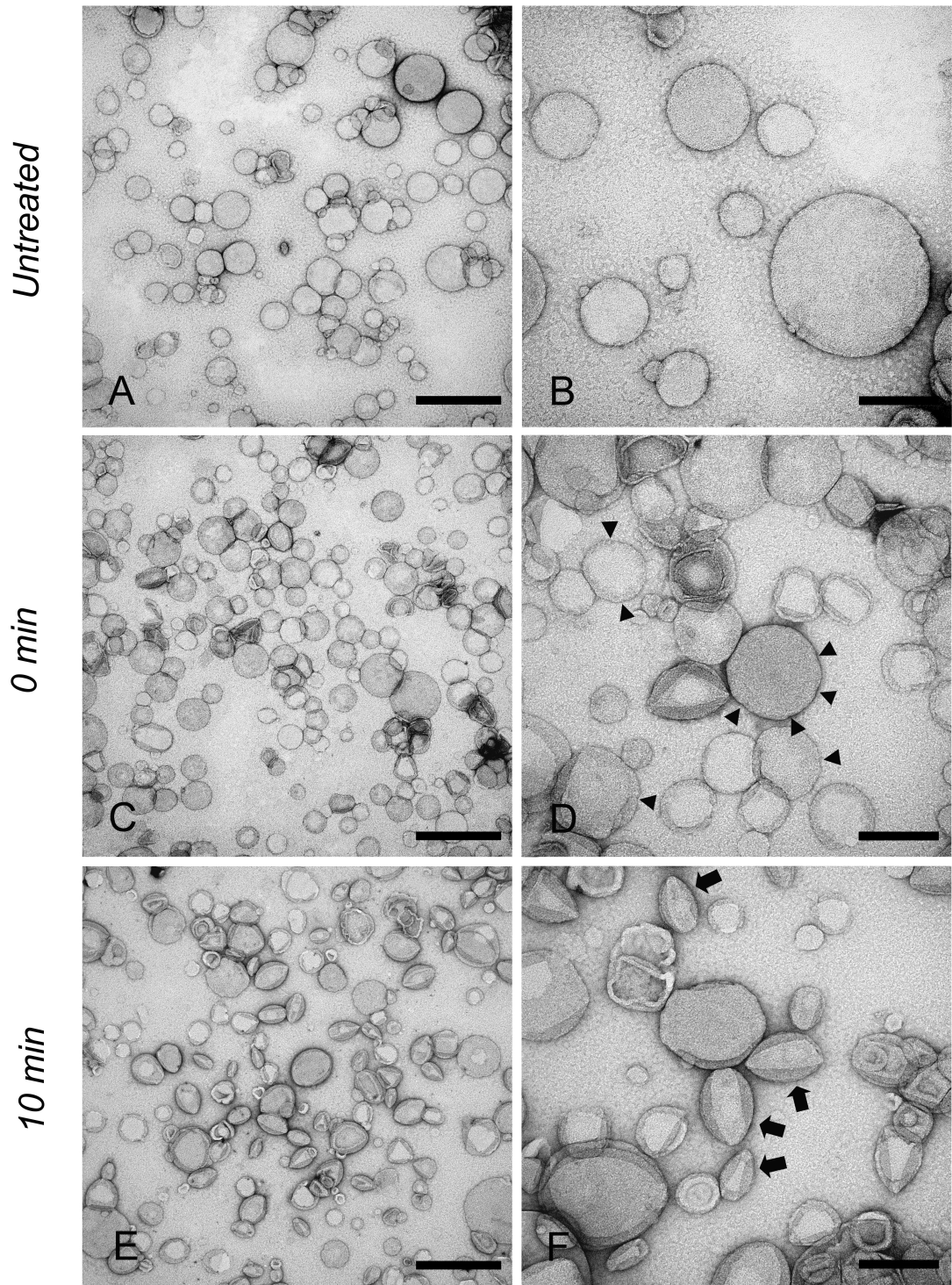
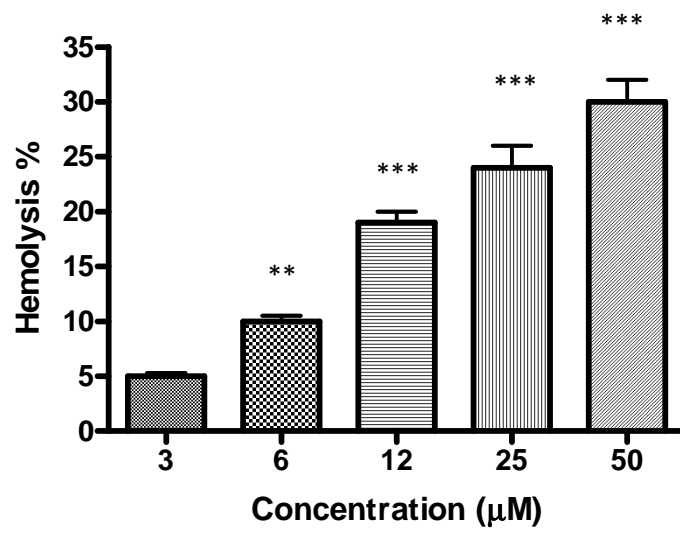


Figure 6

Figure 7.



Highlights

- 1) Fish antimicrobial peptides are relevant as new possible antibiotics
- 2) A new fish-derived antimicrobial peptide has been designed
- 3) Its interactions with bacterial membranes have been investigated in detail
- 4) The peptide shows high antimicrobial activity against known pathogenic Gram – bacteria